Figure 4 shows a universal plot of reduced expansion factor $\alpha(N/N_C)^{1/6}$ vs reduced blob size (N/N_C). The experimental data for light scattering studies yielded α_s and α_h and were transferred from Figure 14 of ref 1 and Figure 6 of ref 11, respectively, and α_h in the collapsed regime also from Figure 2 of ref 3. In Figure 4, an experimental ratio of $\alpha_h^3:\alpha_\eta^3:\alpha_s^3 = 2.14 \pm 0.19:1.2 \pm 0.1:1$ was obtained. We noted that $\alpha_h\alpha_s^2$ as $\alpha_\eta^3/\alpha_s^2\alpha_h = 24.1/25.6 \simeq 1$, while if we take an average of the two data sets (present work and ref 9) $(\alpha_\eta^3|\tau|M_w^{1/2})_{plateau} = 25.6$, we have $\alpha_\eta^3/\alpha_s^2\alpha_h \simeq 25.6/25.6 = 1$ or $\alpha_\eta^3 = \alpha_s^2\alpha_h$. It should be noted that there is one true value for α_η and we should not really add the two data sets. By averaging the two data sets, we merely point out that the expansion factors contain fairly large experimental uncertainties.

Acknowledgment. We gratefully acknowledge support of this work by the National Science Foundation, Polymer Program (DMR 8617820).

Registry No. Polystyrene, 9003-53-6; cyclohexane, 110-82-7.

References and Notes

(1) Park, I. H.; Wang, Q.-W.; Chu, B. *Macromolecules* **1987**, *20*, 1965, and references therein.
(2) Chu, B.; Park, I. H.; Wang, Q.-W.; Wu, C. *Macromolecules* **1987**, *20*, 2833.
(3) Chu, B.; Xu, R. L.; Zuo, J. *Macromolecules* **1988**, *21*, 273.
(4) Chu, B. *Transition of Linear Polymer Dimension from Theta to Collapsed Regime*; Proceedings of International Symposium on Dynamics of Ordering Processes, Kyoto, Japan, 1987, in press.
(5) Chu, B.; Xu, R. L.; Wang, Z.-L.; Zuo, J. *J. Appl. Crystallogr.*, in press.
(6) Chu, B.; Wang, Z.-L. *Macromolecules* **1988**, *21*, 2283.
(7) Sanchez, I. C. *J. Appl. Phys.* **1985**, *58*, 2871.
(8) Dhadwal, H. S.; Chu, B.; Wang, Z.-L.; Kocka, M.; Blumrich, M. *Rev. Sci. Instrum.* **1987**, *58*, 1494.
(9) Perzynski, R.; Delsanti, M.; Adam, M. *J. Phys. (Les Ulis, Fr.)* **1984**, *45*, 1765.
(10) Park, I.-H.; Fetters, L.; Chu, B. *Macromolecules* **1988**, *21*, 1178.
(11) Vidakovic, P.; Rondelez, F. *Macromolecules* **1984**, *17*, 418.
(12) Daoud, M.; Jannink, G. *J. Phys. (Les Ulis, Fr.)* **1978**, *39*, 331.
(13) Farnoux, B.; et al. *J. Phys. (Les Ulis, Fr.)* **1978**, *39*, 77.

Determination of the Order–Disorder Transition Temperature of Block Copolymers

Chang Dae Han,* Jinhwan Kim, and Jin Kon Kim

Department of Chemical Engineering and Polymer Research Institute, Polytechnic University, Brooklyn, New York 11201. *Received November 9, 1987; Revised Manuscript Received May 20, 1988*

ABSTRACT: The order–disorder transition temperature (T_r) of two commercial block copolymers, a polystyrene-*block*-polybutadiene-*block*-polystyrene (SBS) (Kraton 1102, Shell Development Co.) and a polystyrene-*block*-polyisoprene-*block*-polystyrene (SIS) (Kraton 1107, Shell Development Co.), was determined, by using a rheological technique recently suggested by Han and Kim. The rheological technique calls for measurements of dynamic viscoelastic properties, namely, storage modulus $G'(\omega)$ and loss modulus $G''(\omega)$ as a function of angular frequency (ω) under isothermal conditions. It has been observed that log G' versus log G'' plots for the block copolymers investigated vary with temperature up to a certain critical value and then become *virtually* independent of temperature as the temperature increases further. Therefore the critical temperature at which log G' versus log G'' plots cease to vary with temperature is regarded as T_r. Our experimental results indicate that, to within ±10 °C, the T_r of Kraton 1102 is 220 °C and the T_r of Kraton 1107 is 230 °C. The currently held theories of Helfand–Wasserman and Leibler were used to predict the T_r's of the block copolymers investigated. It has been found that the accuracy of the theoretical predictions of T_r depends very much on the accuracy of the temperature dependency of both the interaction parameter and the specific volumes of the constituent components in a block copolymer.

Introduction

It is a well-established fact today that diene-based block copolymers, such as polystyrene-*block*-polybutadiene (SB), polystyrene-*block*-polybutadiene-*block*-polystyrene (SBS), and polystyrene-*block*-polyisoprene-*block*-polystyrene (SIS), have an ordered microdomain structure in the form of spheres, cylinders, or lamellae, depending upon the proportions of the constituent components.[1,2] However, as the temperature is raised above a certain critical value, the microdomain structure disappears completely, giving rise to a disordered homogeneous phase. The temperature at which the microdomain structure completely disappears is referred to as the order–disorder transition (also referred to as the microphase separation transition (MST)) temperature (T_r). In recent years, several research groups[3–12] have investigated the order–disorder transition behavior of block copolymers. Some investigators[3–5] conducted theoretical studies while others[6–12] carried out experimental studies.

Leibler[4] has developed a theory, suggesting that small-angle X-ray or neutron scattering techniques be used to investigate the order–disorder transition behavior of block copolymers. Apparently, Leibler's theory has encouraged some investigators[8–11] to use small-angle X-ray scattering (SAXS) and others[12] to use small-angle neutron scattering (SANS) to investigate the order–disorder transition behavior of diene-based block copolymers. They reported that the maximum scattered intensity present at room temperature persists well above the glass transition temperature of the polystyrene domains but disappears at a critical temperature at which the block polymer is believed to become a homogeneous phase.

In the past, the rheological behavior of SB, SBS, and SIS block copolymers at temperatures above the glass transition temperature of the styrene domains was studied extensively by a number of investigators.[13–17] By applying frequency–temperature superposition to their dynamic viscoelastic data, some investigators[13,14] have reported that logarithmic plots of dynamic viscosity (η') versus angular frequency (ω) or logarithmic plots of dynamic storage modulus (G') versus ω for an SB, SBS, or SIS block copolymer show an abrupt change over a narrow temperature

0024-9297/89/2222-0383$01.50/0

range and attributed this phenomenon to the disappearance of the microdomain structure initially present in the block copolymer sample.

Very recently, however, we have pointed out that log $\eta'(\omega)$ versus log ω or log $G'(\omega)$ versus log ω plots are not sensitive enough to accurately determine the T_r of block copolymers and suggested that log G' versus log G'' plots be used to determine the T_r of a block copolymer.[18] This suggestion was based on the experimental observations that log G' versus log G'' plots for an SIS block copolymer varied gradually with increasing temperature up to a certain critical value and then became virtually independent of temperature as the temperature increased further, whereas log G' versus log G'' plots for flexible homopolymers in the molten state were *virtually* independent of temperature over a wide temperature range. Thus we have suggested that the T_r of a block copolymer be determined by the temperature at which log G' versus log G'' plots cease to vary with temperature. We have pointed out further that use of frequency–temperature superposition to block copolymers is inappropriate in the temperature range where morphological changes of the block copolymer may occur, specifically in the temperature range from the glass transition temperature (T_g) of the polystyrene phase to the temperature at which the polystyrene microdomains in the block copolymer are completely destroyed.

Earlier, Han and co-workers[19–23] showed that log G' versus log G'' plots for flexible homopolymers, compatible polymer blends, and graft copolymers in the molten state are virtually independent of temperature. It should be mentioned that in 1941 Cole and Cole[24] first used the ordinary coordinate system to plot the real part (ϵ') of the complex dielectric constant on the abscissa against the imaginary part (ϵ'') on the ordinate, for a number of polar materials at various temperatures. The Cole–Cole plot falls on a circular arc and a different arc is observed for each temperature, with the shape of the circular arc varying with temperature. For a given set of experimental data for dynamic moduli G' and G'' as functions of angular frequency ω, the use of the logarithmic coordinates, instead of the ordinary coordinates, does not change the characteristics of the data, but the sensitivity of log G' versus log G'' plots to temperature becomes very much suppressed. This can be illustrated best, using the analysis of Han and Jhon,[23] as briefly summarized below.

Using the tube model of Doi and Edwards,[25] in oscillatory shearing flow of entangled, monodisperse flexible polymers in the molten state we obtain the following expressions for $G'(\omega)$ and $G''(\omega)$:

$$G'(\omega) = \frac{8}{\pi^2} G_0 \sum_{\substack{\text{odd} \\ p}} \frac{1}{p^2} \frac{(\omega\lambda_p)^2}{1 + (\omega\lambda_p)^2} \tag{1}$$

and

$$G''(\omega) = \frac{8}{\pi^2} G_0 \sum_{\substack{\text{odd} \\ p}} \frac{1}{p^2} \frac{\omega\lambda_p}{1 + (\omega\lambda_p)^2} \tag{2}$$

where $\lambda_p = \tau_p/p^2$ ($p = 1, 3, 5, \ldots$) in which $\tau_p = L^2/D\pi^2$ is the disengagement time, where L is a contour length and D is the curvilinear diffusion constant, and G_0 is a constant. For linear polymers, G_0 can be equated, as a first approximation, to the plateau modulus G_N°, i.e.

$$G_0 = G_N^\circ = \rho RT/M_e \tag{3}$$

where ρ is the density, R is the universal gas constant, T is the absolute temperature, and M_e is the entanglement molecular weight.

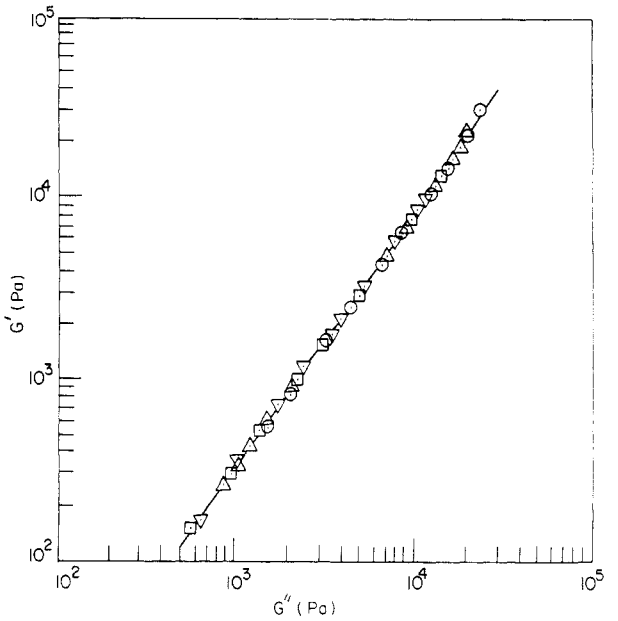

Figure 1. log G' versus log G'' plots for a low-density polyethylene at various temperatures (°C): (⊙) 160; (▲) 200; (⊡) 220; (▽) 238.

It can be shown that in the terminal region (i.e., $\omega\lambda_p \ll 1$) eq 1 and 2, with the aid of eq 3, reduce to[26]

$$G' = (6/5)(M_e/\rho RT)(G'')^2 \tag{4}$$

Taking logarithms of both sides of eq 4, one obtains

$$\log G' = 2 \log G'' + \log (M_e/\rho RT) + \log (6/5) \tag{5}$$

It can be seen from eq 5 that in the terminal region, log G' for monodisperse flexible polymers is proportional to log G'' with a slope of 2, independent of molecular weight, and that the temperature has a very *weak* effect on log G' versus log G'' plots. Note in eq 5 that an increase in temperature from T_1 to T_2 will shift the value of log G' by the amount log (T_1/T_2) and thus, for instance, an increase in temperature from 180 to 240 °C will shift the value of log G' by the amount 0.054. Such an insignificant amount of shift in log G' will hardly be noticeable in the log G' versus log G'' plots.

The above point is illustrated in Figure 1 for a low-density polyethylene over the temperature range 160–238 °C. It can be seen in Figure 1 that log G' versus log G'' plots do not show temperature dependence over the temperature range from 160 to 238 °C. Similar observations have been reported for many other flexible polymer systems.[19–23] Note that the slope of the log G' versus log G'' plots in Figure 1 is less than 2 over the range of G'' investigated, while eq 5 predicts that the slope of log G' versus log G'' plots should be 2. There are two reasons why the slope of the log G' versus log G'' plot in Figure 1 is less than 2. The first reason is that the range of frequency ω (or G'') investigated was not sufficiently low to have reached the terminal region, where the slope of all materials must be 2. Note that for the LDPE investigated, being a very high molecular weight polymer, it was practically very difficult, if not impossible, to have the frequency sufficiently low to reach the terminal region. The second reason is due to the polydispersity of the LDPE investigated. If the LDPE were monodisperse, its log G' versus log G'' plots would have had a slope of 2 over the range of G'' investigated.

Theoretical Background

Several research groups[3,4,27–31] have developed theories which enable one to predict the order–disorder transition

temperature (T_r) of block copolymers. Using a mean-field theory, Helfand[27,28] and Helfand and Wasserman[3,29] developed a statistical thermodynamic theory to predict the free energy and domain size of block copolymer systems. Using this theory, Helfand and Wasserman[3] made an attempt to predict the T_r of SB and SBS block copolymers. On the basis of a random phase approximation method due to de Gennes,[32] Leibler[4] developed a theory to predict the microphase separation transition in block copolymers, which also enabled him to predict the T_r of AB-type diblock copolymers. In this section we will review briefly Helfand–Wasserman's and Leibler's theories of block polymers, only to the extent that they will enable us to compute the phase transition temperature of the block copolymers that were investigated in this study.

The Helfand–Wasserman Theory. In a series of papers.[3,29] Helfand and Wasserman derived expressions for the free energy of AB- and ABA-type block copolymer systems having a spherical, cylindrical, or lamellar microdomain structure. According to Helfand and Wasserman,[3,29] the difference in free energy density $\mathcal{E}$ of a block copolymer between the state with microdomain structure and the state with homogeneous phase is given by

$$\mathcal{E} = \mathcal{E}_B - \mathcal{E}_H \tag{6}$$

where $\mathcal{E}_B$ is the free energy density of a block copolymer with microdomain structure and $\mathcal{E}_H$ is the free energy density of the block copolymer in the homogeneous state. Note that $\mathcal{E}_B$ consists of three contributions:

$$\mathcal{E}_B = \mathcal{E}_S + \mathcal{E}_J + \mathcal{E}_D \tag{7}$$

where $\mathcal{E}_S$ denotes the surface free energy density that has two contributions, one from the interfacial tension between homopolymers A and B and the other from the surface-to-volume ratio, which is inversely proportional to the domain size; $\mathcal{E}_J$ denotes the loss of entropy, which is proportional to the logarithm of the ratio of the density of joints in the interphase to the density of joints in the homogeneous system; and $\mathcal{E}_D$ denotes the loss of conformational entropy in maintaining uniform density in the A and B domains.

The Helfand–Wasserman theory can be summarized in the following general form:[33]

$$\mathcal{E} = \mathrm{Sh}\left(\frac{N_A}{\rho_{0A}}\right)\left(\frac{\gamma}{k_BT}\right)\frac{1}{X} + \ln\left(\frac{XT_1}{\mathrm{Sh}a_J}\right) + [\eta_{A1}(C_2X^2 + \eta_{A2}^2)^{\eta_{A3}/2} - \eta_{A1}(\eta_{A2})^{\eta_{A3}}] + [\eta_{B1}(C_6X^2 + \eta_{B2}^2)^{\eta_{B3}/2} - \eta_{B1}(\eta_{B2})^{\eta_{B3}}] - \alpha\frac{(N_A/\rho_{0A})(N_B/\rho_{0B})}{(N_A/\rho_{0A} + N_B/\rho_{0B})} \tag{8}$$

where

$$C_2 = 6/N_Ab_A^2; \qquad C_6 = 6/N_Bb_B^2\xi^2 \tag{9}$$

where

$$1/\xi = \left(\frac{N_A/\rho_{0A}}{N_B/\rho_{0B}} + 1\right)^{1/\mathrm{Sh}} - 1 \tag{10}$$

in which Sh is a shape factor (1 for lamellar structure, 2 for cylindrical structure, and 3 for spherical structure); N_A and N_B are the degrees of polymerization for components A and B, respectively, where N_B must be replaced by $N_B/2$ for triblock copolymers; ρ_{0A} and ρ_{0B} are the densities of pure components A and B, respectively, expressed in terms of monomer segments per unit volume; γ is the interfacial tension; k_B is the Boltzmann constant; T is the absolute temperature; X is the domain size; T_1 is related to the shape factor (Sh) and the degree of polymerization (N_A and N_B); η_{A1}, η_{A2}, η_{A3}, η_{B1}, η_{B2}, and η_{B3} are parameters which depend upon the microdomain structure of the block copolymer, the numerical values of which are summarized in Table I; α is the interaction parameter; and a_J depends on β_A, β_B, and α

Table I
Numerical Values for the Parameters Appearing in Helfand-Wasserman's Theory (See Equation 8)

param	cylindrical domain	spherical domain
η_{A1}	0.0274	0.0123
η_{A2}	0.202	0.384
η_{A3}	2.605	2.680
η_{B1}	$0.0659 + 0.0357/\xi$	$0.0705 + 0.0578/\xi$
η_{B2}	$0.757 - 0.132/\xi$	$0.596 + 0.599/\xi$
η_{B3}	$2.590 - 0.147/\xi$	$2.550 - 0.132/\xi$

$$a_J = f(\beta_A,\beta_B)/\alpha^{1/2} \tag{11}$$

where

$$\beta_A = \rho_{0A}b_A/6; \qquad \beta_B = \rho_{0B}b_B/6 \tag{12}$$

in which b_A and b_B are the Kuhn statistical lengths of components A and B, respectively. Note that γ/k_BT in eq 8 is given by[34]

$$\frac{\gamma}{k_BT} = \alpha^{1/2}\left\{\left(\frac{\beta_A + \beta_B}{2}\right) + \frac{1}{6}\frac{(\beta_A - \beta_B)^2}{(\beta_A + \beta_B)}\right\} \tag{13}$$

According to Helfand and Wasserman,[3,29,33] the value of T_r can be determined by finding the temperature at which the free energy density given by eq 8 becomes zero, i.e.

$$\mathcal{E}(X^*) = 0 \tag{14}$$

where X^* is the domain size that satisfies

$$d\mathcal{E}/dX = 0 \tag{15}$$

i.e.

$$-\mathrm{Sh}\left(\frac{N_A}{\rho_{0A}}\right)\left(\frac{\gamma}{k_BT}\right) + X^* + [\eta_{A1}\eta_{A3}C_2(C_2X^{*2} + \eta_{A2}^2)^{[(\eta_{A3}/2)-1]}X^{*3}] + [\eta_{B1}\eta_{B3}C_6(C_6X^{*2} + \eta_{B2}^2)^{[(\eta_{B3}/2)-1]}X^{*3}] = 0 \tag{16}$$

Note that the interaction parameter α depends on temperature, thus a_J (see eq 11) and γ/k_BT (see eq 13) also depend on temperature. The computational procedure to determine T_r is as follows: (1) Assume a value for temperature and evaluate all necessary parameters (α, a_J, γ, etc.); (2) solve eq 16 for X^*; (3) substitute the value X^* into eq 8 to evaluate the free energy density $\mathcal{E}$. If the free energy density evaluated is not equal to zero (i.e., if eq 14 is not satisfied), assume a new value for temperature and repeat the process until eq 14 is satisfied and, then, one will have the equilibrium domain size X_{eq} and T_r.

The Leibler Theory. Leibler[4] derived the following expression for the composition correlation function $\tilde{S}(q)$ for a block copolymer:

$$\tilde{S}(q) = W(q)/[S(q) - 2\chi W(q)] \tag{17}$$

where q is the wave vector, χ is the interaction parameter, and $S(q)$ and $W(q)$ are defined by

$$S(q) = S_{11}(q) + S_{22}(q) + 2S_{12}(q) \tag{18}$$

$$W(q) = S_{11}(q)S_{22}(q) - S_{12}^2(q) \tag{19}$$

in which $S_{ij}(q)$ are the elements of the matrix $\|S(q)\|$, which is the Fourier transform of the composition correlation functions for the ideal independent copolymer chains.

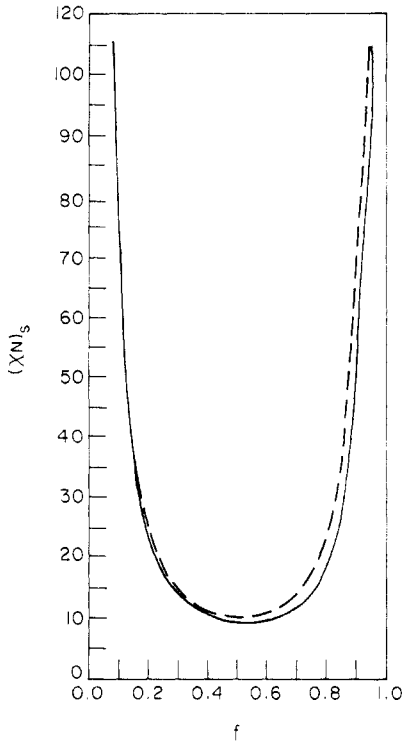

Figure 2. $(\chi N)_s$ versus f plots, in which f is f_1 for diblock copolymer and $2f_1$ for triblock copolymer. The broken curve represents AB-type diblock copolymer and the solid curve represents ABA-type triblock copolymer.

The composition correlation functions $S_{ij}(q)$ for an AB-type *diblock* copolymer are given by[4]

$$S_{11}(q) = Ng_1(f_1,x) \tag{20}$$

$$S_{22}(q) = Ng_1(1-f_1,x) \tag{21}$$

$$S_{12}(q) = (N/2)[g_1(1,x) - g_1(f_1,x) - g_1(1-f_1,x)] \tag{22}$$

where f_1 is the fraction of block A (or block B) in an AB-type diblock copolymer for which $f_1 + f_2 = 1$, N is the polymerization index of the block copolymer, and $g_1(f_1,x)$ is the Debye function defined as

$$g_1(f_1,x) = (2/x^2)[f_1x + \exp(-f_1x) - 1] \tag{23}$$

and x is defined by

$$x = q^2Na^2/6 = q^2R_g^2 \tag{24}$$

where q is the wave vector, a is the statistical segment length for blocks A and B (assumed to be identical), and R_g is the radius of gyration of an ideal chain.

Leibler[4] has shown that the use of eq 18–22 in eq 17 gives

$$\tilde{S}(q) = N/[F(x) - 2\chi N] \tag{25}$$

where

$$F(x) = g_1(1,x)/\{g_1(f_1,x)g_1(1-f_1,x) - (1/4)[g_1(1,x) - g_1(f_1,x) - g_1(1-f_1,x)]^2\} \tag{26}$$

Here, one can obtain a relationship between $(\chi N)_s$, at which spinodal decomposition occurs, and f_1, by finding values of x^* (or q^*) that make $\tilde{S}(q)$ a maximum. Such relationships for diblock copolymers are given by the *broken* curve, representing a thermodynamic stability limit, in Figure 2, in which the region below the U-shaped curve represents the thermodynamically stable and metastable phases, while the region inside the curve represents the mesophase (i.e., microphase-separated phase). Note in Figure 2 that χ is dependent upon the composition f and is inversely proportional to temperature, and therefore, at a given value of f, with information on N the spinodal decomposition temperature (T_s) can be determined from the value of $(\chi N)_s$. Leibler has shown further that the microdomain structure (lamellar, cylindrical, or spherical) of the ordered phase influences the value of T_s. Figure 3 displays relationships between transition temperature in terms of χN and f_1 for a diblock copolymer with different microdomain structures. According to Figures 3, a transition from a disordered phase to a lamellar microdomain structure at $f = 0.2$, for instance, by decreasing the temperature, passes through the spherical microdomain structure and then the cylindrical microdomain structure. However, this theoretical prediction has yet to be confirmed experimentally.

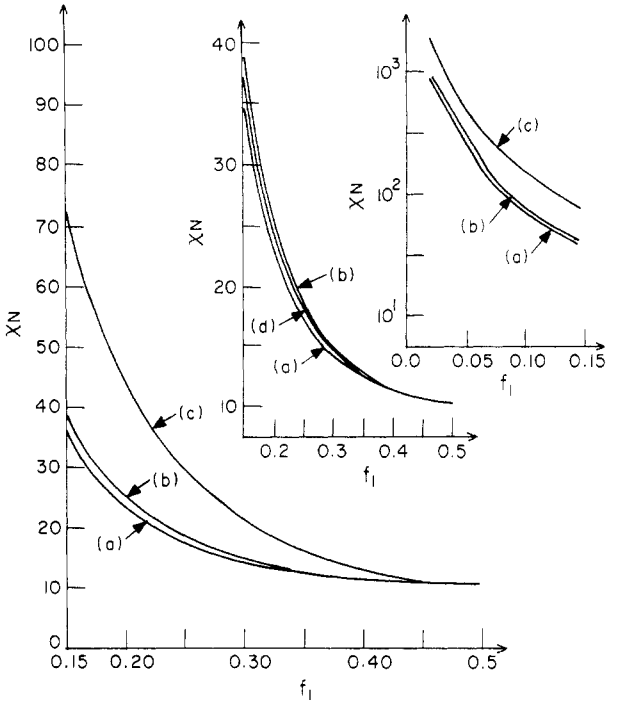

Figure 3. χN versus f_1 plots for diblock copolymers:[4] (a) phase transition from the disordered phase to spherical microdomain structure; (b) phase transition from spherical to cylindrical microdomain structure; (c) phase transition from cylindrical to lamellar microdomain structure; (d) spinodal curve ($(\chi N)_s$ versus f_1).

It should be mentioned that Helfand's theory is valid for a strong segregation limit and therefore for the formation and dissolution of a fully developed domain system, whereas Leibler's theory is valid for a weak segregation limit and therefore for the onset conditions of the domain formation or for the final step of the domain dissolution.

Very recently, by including composition fluctuations which were neglected in Leibler's analysis, Fredrickson and Helfand[5] investigated the phase transition behavior of a diblock copolymer and concluded that (1) for a symmetric diblock copolymer (i.e., $f = 0.5$) with finite values of N, Leibler's prediction, $(\chi N)_s = 10.495$, must be modified by

$$(\chi N)_t = 10.495 + 41.022N^{-1/3} \tag{27}$$

where $(\chi N)_t$ refers to the location of the transition (MST) induced by composition fluctuations, and (2) it is possible to pass from the disordered phase to each of the ordered microphases (lamellar, cylindrical, and spherical microdomain structures) by changing the temperature.

The composition correlation functions $S_{ij}(q)$ for an ABA-type *triblock* copolymer are given by Mori et al.[35]

$$S_{11}(q) = N[g_1(f_1,x) + g_1(f_2,x) + g_1(f_3,x) + g_1(1,x) - g_1(1-f_3,x) - g_1(1-f_1,x)] \tag{28}$$

$$S_{22}(q) = Ng_1(f_2,x) \quad (29)$$

$$S_{12}(q) = (N/2)[g_1(1-f_1,x) + g_1(1-f_3,x) - g_1(f_1,x) - g_1(f_3,x) - 2g_1(f_2,x)] \quad (30)$$

where f_1, f_2, and f_3 are the volume fractions of each block sequence in an ABA-type triblock copolymer, for which $f_1 + f_2 + f_3 = 1$. Note that when $f_3 = 0$, eq 28–30 reduce to eq 20–22.

For an ABA-type triblock copolymer, $f_1 = f_3$ and therefore A – (1/2)B may be considered to be equivalent to a diblock copolymer obtained by cutting the ABA triblock copolymer in the middle of B. It would be interesting to see how close the spinodal point of the A – (1/2)B diblock copolymer predicted by eq 20–22 comes to that of the ABA triblock copolymer predicted by eq 28–30. For comparison purposes, relationships between $(\chi N)_s$ and f for an ABA-type triblock copolymer are given by the *solid* curve in Figure 2. It can be seen in Figure 2 that the predictions of $(\chi N)_s$ for the two cases, AB-type diblock and ABA-type triblock copolymers, become very close only when f is equal to or less than approximately 0.2. This has been extensively discussed by Mori et al.[35]

Experimental Section

Two block copolymers of commercial grade, a polystyrene-*block*-polybutadiene-*block*-polystyrene (SBS) (Kraton D-1102, Shell Development Co.) and a polystyrene-*block*-polyisoprene-*block*-polystyrene (SIS) (Kraton D-1107, Shell Development Co.), were investigated. These block copolymers have segment molecular weights[36] 10 000 S–50 000 B–10 000 S for Kraton 1102 and 10 000 S–120 000 I–10 000 S for Kraton 1107, and each of the block copolymers contains about 20 wt % uncoupled diblock.

Samples for rheological measurement were prepared by first dissolving the block copolymer in toluene (10% of solid in solution) followed by solvent evaporation. The evaporation of solvent was carried out initially in open air at room temperature for a week and then in a vacuum oven at 40 °C for 3 days. The last trace of solvent was removed by drying the sample in a vacuum oven at an elevated temperature by gradually raising the oven temperature up to 110 °C. The drying of the sample was continued until there was no further change in weight. Finally, the sample was annealed at 130 °C for 10 h.

A cone-and-plate rheometer (Weissenberg Model R-16 Rheogoniometer) was used to measure the dynamic storage modulus (G') and loss modulus (G'') as a function of angular frequency (ω) in the oscillatory shear mode, under isothermal conditions. The diameter of the platen was 25 mm and the cone angle was 4°. Data acquisition was accomplished with the aid of a microcomputer interfaced with the rheometer. Rheological measurements were made at temperatures over the range 140–240 °C. Measurements at temperatures above 240 °C were not possible, due to thermal degradation of the samples. The temperature control of the rheometer was satisfactory to within ±1 °C. For each rheological measurement, a fixed strain was used at a given temperature. Specifically, the strain was varied from 0.03% at 140 °C to 0.3% at 240 °C, which were well within the linear viscoelastic range of the materials investigated. All experiments were conducted under a nitrogen blanket in order to avoid oxidative degradation of the samples.

Experimental Results

Figure 4 gives log G' versus log ω plots and Figure 5 log G'' versus log ω plots, for Kraton 1102 at eight different temperatures: 160, 180, 190, 200, 210, 220, 230, and 240 °C. It is seen in Figure 4 that at temperatures of 200 °C and below, G' increases modestly with increasing ω, behavior typical of cross-linked polymers, but at temperatures above 200 °C the slope of log G' versus log ω curves at low values of ω becomes steep, behavior typical of homogeneous thermoplastic melts.[37] It is seen in Figure 5 that the dependencies of G'' on ω and temperature look very similar to the dependencies of G' on ω and temperature, observed in Figure 4. Figure 6 gives log G' versus log G'' plots for Kraton 1102, which were prepared with the data from Figures 4 and 5. It is seen in Figure 6 that at a fixed value of G'', G' varies little with temperature in the range 160–200 °C, then suddenly decreases as the temperature is increased from 200 to 220 °C, and then remains *virtually* constant, independent of temperature, at 220 °C and above. In other words, for Kraton 1102, 220 °C is the lowest temperature at which log G' versus log G'' plots cease to vary with temperature.

Figure 7 gives log G' versus log ω plots and Figure 8 log G'' versus log ω plots, for Kraton 1107 at 11 different temperatures: 140, 148, 160, 170, 180, 190, 200, 210, 220, 230, and 240 °C. It is seen in Figures 7 and 8 that values of G' and G'' for Kraton 1107 decrease gradually as the temperature is increased from 140 to 240 °C, without showing any abruptness that was observed in Figures 4 and 5. Using the data from Figures 7 and 8, log G' versus log

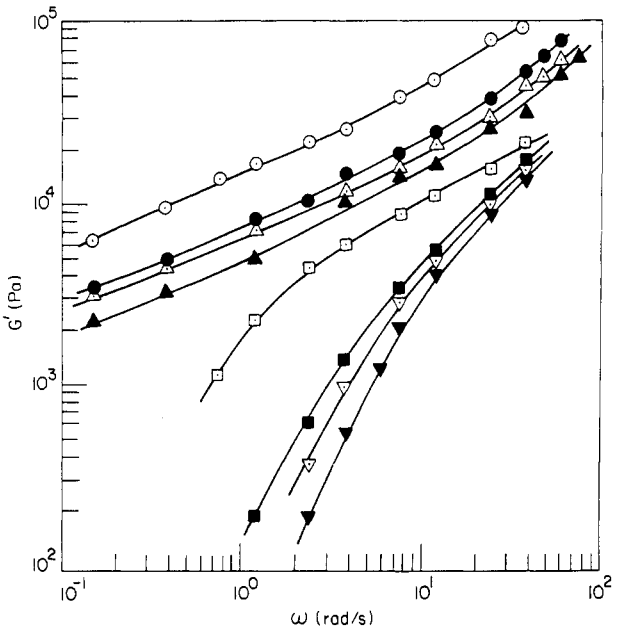

Figure 4. log G' versus log ω plots for Kraton 1102 at various temperatures (°C): (⊙) 160; (●) 180; (△) 190; (▲) 200; (□) 210; (■) 220; (▽) 230; (▼) 240.

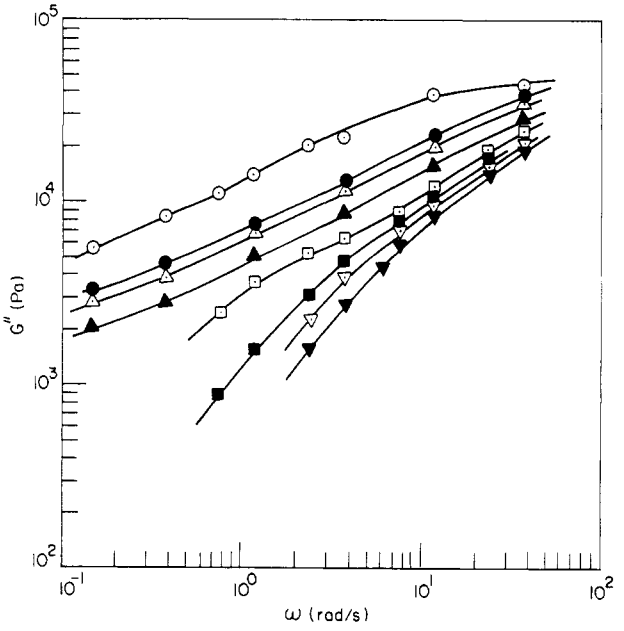

Figure 5. log G'' versus log ω plots for Kraton 1102 at various temperatures. Symbols are the same as in Figure 4.

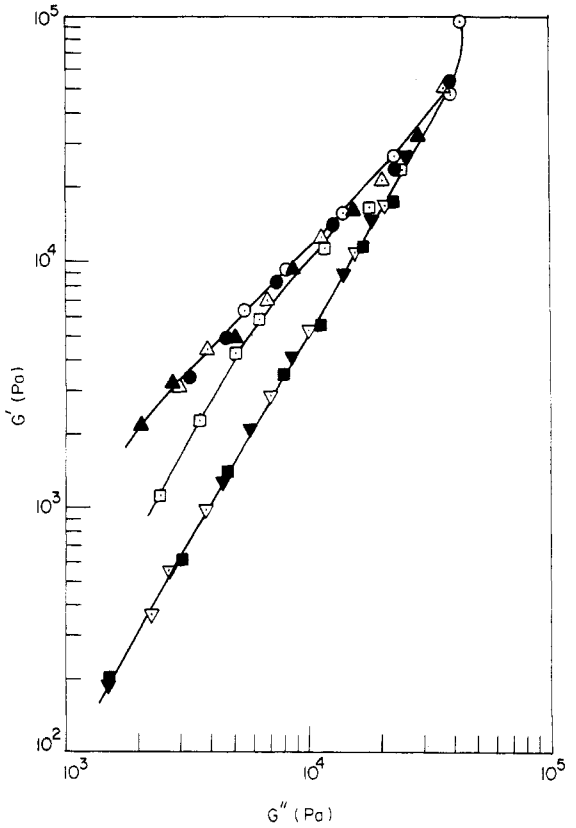

Figure 6. log G' versus log G'' plots for Kraton 1102 at various temperatures. Symbols are the same as in Figure 4.

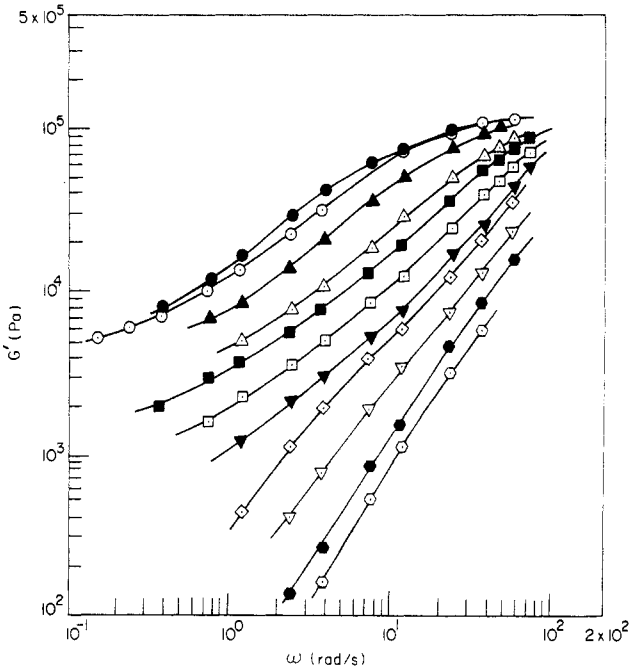

Figure 7. log G' versus log ω plots for Kraton 1107 at various temperatures (°C): (●) 140; (⊙) 148; (▲) 160; (◬) 170; (■) 180; (⊡) 190; (▼) 200; (◈) 210; (▽) 220; (●) 230; (⊙) 240.

G'' plots were prepared and are given in Figure 9. In contrast to the situation observed for Kraton 1102 in Figure 6, it is seen in Figure 9 that for Kraton 1107, at a fixed value of G'', G' decreases gradually as the temperature is increased from 140 to 230 °C and then remains constant, independent of temperature, at 230 °C and above. In other words, for Kraton 1107, 230 °C is the lowest temperature at which log G' versus log G'' plots cease to vary with temperature.

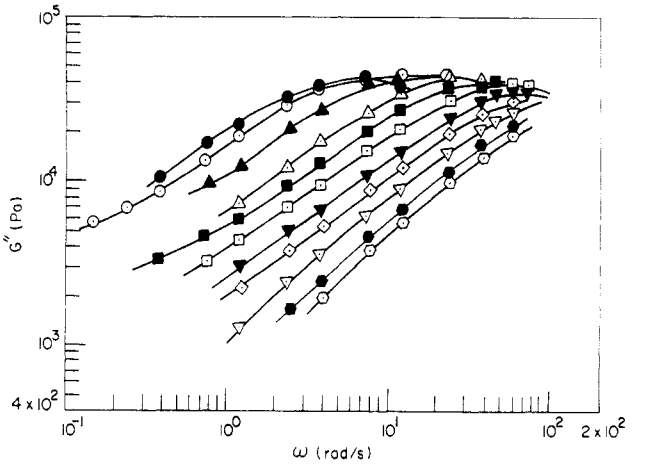

Figure 8. log G'' versus log ω plots for Kraton 1107 at various temperatures. Symbols are the same as in Figure 7.

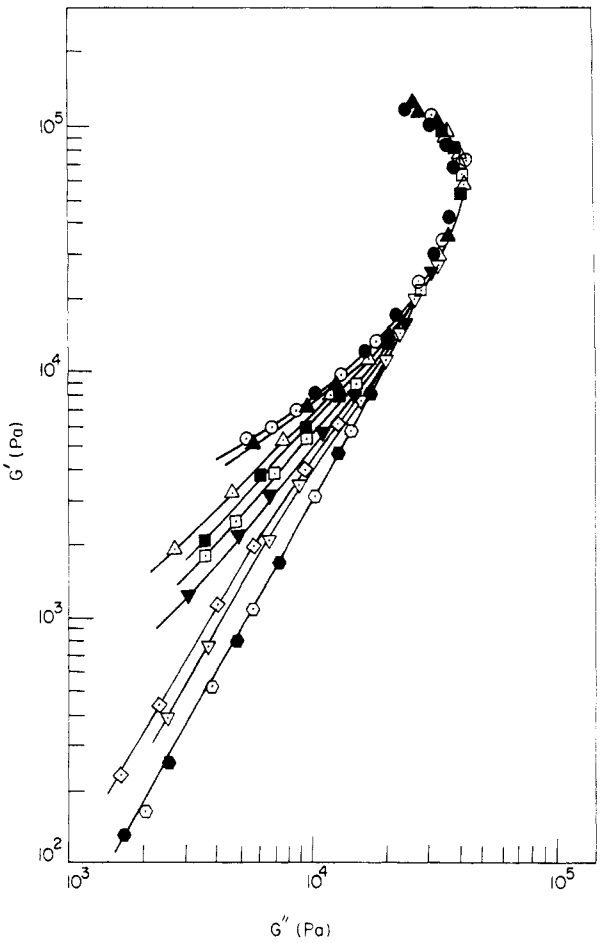

Figure 9. log G' versus log G'' plots for Kraton 1107 at various temperatures. Symbols are the same as in Figure 7.

On the basis of the theoretical prediction by eq 5 that log G' versus log G'' plots for monodisperse flexible homopolymers in the molten state have a very *weak* temperature dependence, we can conclude from Figures 6 and 9 that the *strong* temperature dependence of log G' versus log G'' plots over a certain range of temperatures, observed experimentally for the Kraton 1102 and Kraton 1107, is attributable to the occurrence of a thermally induced transition from an ordered microdomain structure to a disordered homogeneous phase. This conclusion cannot be reached by using log G' versus log ω and log G'' versus log ω plots (i.e., using Figures 4 and 5 for Kraton 1102 and Figures 7 and 8 for Kraton 1107). If there were no or-

der–disorder transition (i.e., no morphological change) occurring in the block copolymers as the temperature was increased from 160 to 240 °C for Kraton 1102 and from 140 to 240 °C for Kraton 1107, we would expect *virtually* no temperature dependence in the log G' versus log G'' plots in Figures 6 and 9 (see Figure 1). It can therefore be concluded that the T_r for Kraton 1102 is 220 °C, and the T_r for Kraton 1107 is 230 °C.

Note that T_r here is defined as the temperature at which the dependence of log G' versus log G'' plots on temperature becomes hardly discernible, i.e., virtually independent of temperature. Very recently, Fredrickson and Larson[38] pointed out that composition fluctuations in the disordered phase at temperatures sufficiently close to MST temperature can lead to strong temperature dependence. Under such circumstances, the values of T_r determined in the present study may not be very accurate.

It should be pointed out that in the use of SAXS by Hashimoto and co-workers[6-8] and Roe and co-workers,[9-11] T_r was determined to be the temperature at which the intensity of the first-order scattering maximum drops to such a level that the first-order peak is hardly discernible. According to Leibler,[4] the reciprocal of the scattering intensity ($1/I$) should be a linear function of the interaction parameter χ. If χ is assumed to be proportional to the reciprocal of the absolute temperature $1/T$, the plot of $1/I$ versus $1/T$ should give a straight line in the disordered state. Hashimoto and co-workers and Roe and co-workers determined T_r to be the temperature at which a linear relationship between $1/I$ and $1/T$ starts to deviate. In the use of SAXS Hashimoto and co-workers[8,39,40] observed further that the characteristic size D of spatial segmental density fluctuations was independent of temperature in the disordered state but dependent upon temperature in the ordered state. They determined T_r to be the temperature at which D starts to vary with temperature.

Comparison of Experimental Results with Theoretical Predictions

Microdomain Structure in Kraton 1102 and Kraton 1107. Before we begin to calculate the order–disorder transition temperature T_r of a block copolymer, we must first have information on the microdomain structure of the block copolymer. Figure 10 gives transmission electron microscope (TEM) photomicrographs of Kraton 1102 and Kraton 1107. Note that the light areas represent the polystyrene microdomains and the dark areas represent the polydiene phase. It can be seen in Figure 10 that Kraton 1102 has a cylindrical microdomain structure and Kraton 1107 has a spherical microdomain structure. The microdomain structures of these block copolymers have also been investigated experimentally by other workers.[2,41-43]

According to Keller and co-workers,[41,42] the SBS block copolymers containing about 30 wt % styrene have a structure consisting of cylindrical polystyrene microdomains in a polybutadiene matrix. Note that Kraton 1102 has segment molecular weights 10 000 S–50 000 B–10 000 S and that the styrene content is about 28 wt %. As may be seen in Figure 10, this block copolymer has a cylindrical microdomain structure.

On the other hand, the segment molecular weights of Kraton 1107 are 10 000 S–120 000 I–10 000 S and the styrene content is about 15 wt %. As may be seen in Figure 10, this block copolymer has a spherical microdomain structure, confirming the results of the previous investigators,[2,43] It should be mentioned that Kraton 1102 and Kraton 1107 contain about 20 wt % uncoupled diblock, which was produced during the anionic polymerization

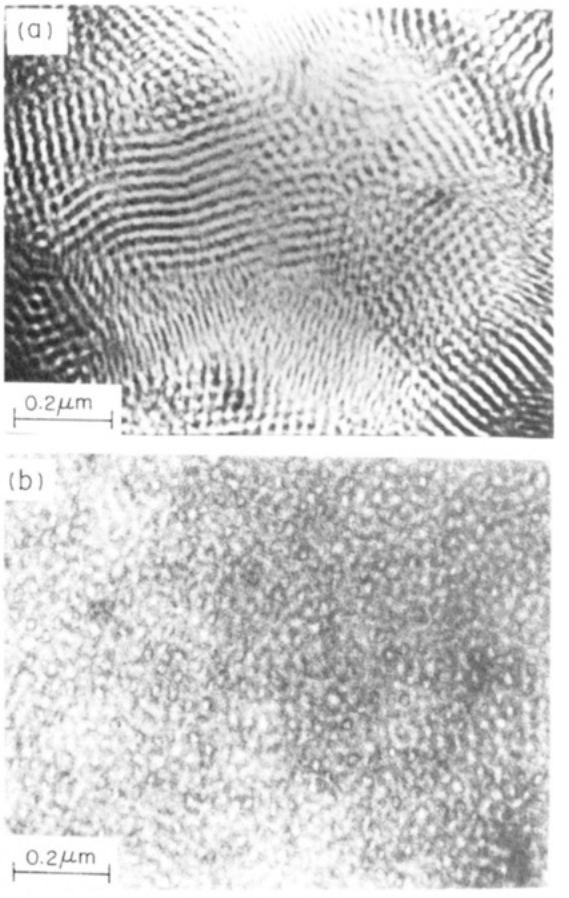

Figure 10. TEM photomicrographs of an ultrathin section, cut parallel to the film surface, of the film cast from toluene: (a) Kraton 1102; (b) Kraton 1107.

followed by a coupling reaction to yield the triblock copolymer, and a small amount of polystyrene homopolymer. According to Fetters et al.,[44] the amount of polystyrene homopolymer in each of these block copolymers is about 1% or less. The presence of the uncoupled diblock and, possibly, the minute amount of polystyrene homopolymer, might be responsible for, according to Fetters et al.,[44] the diffuse phase boundaries between the polystyrene domains and the polydiene matrix, observed in the TEM photomicrographs of Figure 10.

Calculation of the Thermally Induced Transition Temperature of a Block Copolymer. Having experimentally established above that Kraton 1102 has a cylindrical microdomain structure and Kraton 1107 has a spherical microdomain structure, we will now proceed to predict the phase transition temperatures, namely, spinodal decomposition temperature (T_s) and/or order–disorder transition temperature (T_r), of the two block copolymers investigated herein, using the theories summarized above (see the Theoretical Background section). There are a number of molecular and thermodynamic parameters involved with the theories. They are (a) the interaction parameter α (in Helfand–Wasserman's notation) or χ (in Leibler's notation); (2) polymerization index N, which is needed in Leibler's theory; (3) the reference volume V_{ref}, which is needed when information on χ is available; and (4) Kuhn statistical lengths b_k, which are needed in Helfand–Wasserman's theory. In numerical computation, we have used the following values for b_k: (1) b_{PS} = 0.68 nm for polystyrene; (2) b_{PB} = 0.63 nm for polybutadiene; (3) b_{PI} = 0.59 nm for polyisoprene.[45]

(i) Thermally Induced Transition Temperature of Kraton 1102. In computing the thermally induced tran-

Table II
Summary of the Theoretically Predicted Transition Temperature for Kraton 1102

interaction param	diblock		triblock		Kraton 1102[a]
	T_s, °C	T_r, °C	T_s, °C	T_r, °C	T_r, °C
Leibler's Theory					
Λ (eq 31)	269	267	279	277	275
α (eq 32)	297	294	309	306	304
Helfand–Wasserman's Theory					
Λ (eq 31)		214		224	222
α (eq 32)		232		243	241

[a] $T_r = 0.8T_r(\text{triblock}) + 0.2T_r(\text{diblock})$, due to the fact that Kraton 1102 contains 20 wt % uncoupled diblock.

sition temperature for Kraton 1102, we have assumed that the microdomain structure of Kraton 1102 is of cylindrical shape at temperatures above the glass transition temperature (T_g) of polystyrene and used the following two different expressions to describe the polymer–polymer interaction. One is the expression for the interaction energy density Λ for the polystyrene–polybutadiene pair given by Lin and Roe:[46]

$$\Lambda = 1.573 - 0.0021T + 0.09f_{PS} \quad (31)$$

where Λ is expressed in calories per centimeter cubed, T is the absolute temperature, and f_{PS} is the volume fraction of polystyrene in the block copolymer. The other expression used is the interaction parameter α for the pair given by Rounds:[47]

$$\alpha = -900 + 7.5 \times 10^5/T \quad (32)$$

where α is expressed in moles per meter cubed.

In applying Helfand–Wasserman's theory, the relationship $\alpha = \Lambda/RT$ was used to compute α from eq 31. Note that in applying Leibler's theory (see Figure 2), one needs information on χN, but not on χ and N separately. Once values of α are known, values of χN can be calculated from

$$\chi N = \alpha[V_{PS} + V_{PB}] = \alpha[M_{w,PS}v_{PS} + M_{w,PB}v_{PB}] \quad (33)$$

where V_{PS} and V_{PB} are the molar volumes, $M_{w,PS}$ and $M_{w,PB}$ are the molecular weights, and v_{PS} and v_{PB} are the specific volumes of the polystyrene and polybutadiene phases, respectively. In order to compute χN from eq 33, the following temperature-dependent expressions for specific volume of polystyrene[48] were used

$$v_{PS} = 0.9199 + 5.098 \times 10^{-4}t + 2.354 \times 10^{-7}t^2 + (32.46 + 0.1017t)/M_{w,PS} \quad (34)$$

where $M_{w,PS}$ is the molecular weight of polystyrene, and for polybutadiene[49]

$$v_{PB} = 1.1138 + 8.24 \times 10^{-4}t \quad (35)$$

Note in eq 34 and 35 that v_{PS} and v_{PB} are expressed in centimeter cubed per gram and t is the temperature in degrees Celsius.

In the present analysis, eq 31 and 32 were used in Helfand–Wasserman's and Leibler's theories, respectively, to calculate the transition temperatures. Note that Leibler's theory allowed for the calculation of both T_s and T_r. The calculated results are summarized in Table II. It should be pointed out in reference to Table II that, for comparison purposes, T_r and T_s for the diblock were obtained by dividing the molecular weight of the midblock in half (i.e., 10 000 S–25 000 B) and, in applying Leibler's theory, T_r for the triblock was obtained by the following expression:

$$T_r(\text{triblock}) = T_s(\text{triblock}) - T_s(\text{diblock}) + T_r(\text{diblock}) \quad (36)$$

The following observations can be made in Table II: (1) Different expressions for the interaction parameter predict different values of T_r. Specifically, eq 32 predicts a T_r about 30 °C higher than does eq 31. (2) Leibler's theory predicts, when using eq 31, a T_r about 55 °C higher than the measured value, 220 °C. Note that eq 27 corrects Leibler's predictions in the proper direction. (3) Helfand–Wasserman's theory predicts, when using eq 31, a T_r of 222 °C, which is very close to the measured value. Considering the facts that the measured value of T_r is only accurate to within ±10 °C and that there are many assumptions made in the development of the Helfand–Wasserman theory, such close agreement between the two may be considered to be fortuitous. We have found that the accuracy of the theoretical prediction of T_r depends on two other factors: (1) the dependence of the interaction parameter Λ on the composition of block copolymer and (2) the dependence of specific volume on temperature. For instance, we have observed that (1) when the last term, $0.09f_{PS}$, on the right-hand side of eq 31 was neglected, Helfand–Wasserman's theory predicts T_r to be 214 °C, which is about 8 °C lower than the value predicted with inclusion of the term, $0.09f_{PS}$, in Λ, and (2) when constant values of specific volumes, $v_{PS} = 0.9507$ cm^3/g and $v_{PB} = 1.1025$ cm^3/g, were used with eq 31, Helfand–Wasserman's theory predicts the T_r to be 190 °C, which is about 30 °C lower than the value predicted by eq 34 and 35. Thus, it can be concluded that information on the temperature dependence of specific volumes is very important to accurate predictions of T_r.

It should be mentioned that by using the SAXS technique, Zin and Roe[10] have determined the T_r to be about 140 °C for an SB diblock copolymer with segment molecular weights 7500 S–20 500 B. Assuming that the SB diblock copolymer has a spherical microdomain structure and using eq 31, together with eq 34 and 35, we have calculated the T_r to be 221 °C with Leibler's theory and 153 °C with Helfand–Wasserman's theory. Again, we have learned that Leibler's theory overpredicts the T_r as much as 80 °C, while Helfand–Wasserman's theory predicts the T_r reasonably close to the measured value. Note that eq 27 corrects Leibler's predictions in the proper direction. When we assumed that the SB diblock copolymer has a cylindrical microdomain structure, we have calculated the T_r to be 212 °C with Leibler's theory and 158 °C with Helfand–Wasserman's theory.

(ii) Thermally Induced Transition Temperature of Kraton 1107. By assuming that the microdomain structure of Kraton 1107 remains spherical at temperatures above T_g, we have computed thermally induced transition temperatures of Kraton 1107. For the computation, we have used the following expression for the interaction parameter χ for the polystyrene–polyisoprene pair given by Mori et al.:[50]

$$\chi = -0.0937 + 66/T \quad (37)$$

In applying Helfand–Wasserman's theory, from eq 37 we calculated α using the relationship

$$\alpha = \chi/V_{ref} \quad (38)$$

where V_{ref} is a reference volume.

On the other hand, in applying Leibler's theory, the polymerization index N had to be calculated, so that values of χN could be determined. Here, N may be defined by

$$N = \frac{V_{PS} + V_{PI}}{V_{ref}} = \frac{M_{w,PS}v_{PS} + M_{w,PI}v_{PI}}{V_{ref}} \quad (39)$$

Table III
Summary of the Theoretically Predicted Transition Temperature for Kraton 1107

interaction param	diblock T_s, °C	diblock T_r, °C	triblock T_s, °C	triblock T_r, °C	Kraton 1107[a] T_r, °C
Leibler's Theory					
χ/V_{ref}[b]	138	146	142	150	149
χ/V_{ref}[c]	159	167	164	171	170
α (eq 32)	220	233	228	238	237
Helfand–Wasserman's Theory					
χ/V_{ref}[b]		141		144	143
χ/V_{ref}[c]		162		165	165
α (eq 32)		224		231	230

[a] $T_r = 0.8T_r$(triblock) + $0.2T_r$(diblock), due to the fact that Kraton 1107 contains 20 wt % uncoupled diblock. [b] V_{ref} defined by eq 40. [c] V_{ref} defined by eq 41.

There is more than one way of defining V_{ref}. In the present investigation, the following two different definitions for V_{ref} are used:

$$V_{ref} = [M]_S v_{PS} \tag{40}$$

and

$$V_{ref} = [([M]_S v_{PS})([M]_I v_{PI})]^{1/2} \tag{41}$$

where $[M]_S$ and $[M]_I$ are the molecular weights of styrene and isoprene monomer units, respectively. Therefore, the use of V_{ref} defined by eq 40 and 41 respectively in eq 38 and 39 gave rise to two different predictions of transition temperature for each theory applied. We have used, also, eq 32 to predict T_s and T_r with Leibler's theory and T_r with Helfand–Wasserman's theory. Note that the use of eq 32 does not require information on V_{ref} and N, and thus the computational procedure becomes much simplified. The computed results are given in Table III.

In the numerical computations eq 34 was used for the specific volume of polystyrene and the following expression for the specific volume of polyisoprene:[51]

$$v_{PI} = 1.0771 + 7.22 \times 10^{-4}t + 2.46 \times 10^{-7}t^2 \tag{42}$$

where t is the temperature in degrees Celsius.

The following observations can be made in Table III: (1) Two different definitions for V_{ref} lead to different predicted values of T_r. (2) The use of the interaction parameter χ, given by eq 37, underpredicts T_r by as much as 70 °C, compared to the measured value, 230 °C. (3) Using eq 32, Helfand–Wasserman's theory predicts the T_r to be about 230 °C, while Leibler's theory predicts it to be about 237 °C. Again, considering the uncertainties of the measurements to be within ±10 °C and the many assumptions made in the theoretical development, such an excellent agreement between the measured and predicted values of T_r may simply be fortuitous. Nevertheless, it is gratifying to see such an excellent agreement. When constant values of specific volume, $v_{PS} = 0.9507$ cm³/g and $v_{PI} = 1.0796$ cm³/g, were used with eq 32, the predicted value of T_r is about 20 °C lower than the value predicted with the temperature-dependent specific volumes, eq 34 and 42.

Discussion

The Sensitivity of log G' versus log G'' Plots of Block Copolymers to Deformation Rate. Note in Figures 6 and 9 that for higher frequencies (i.e., as G'' is increased to about 3×10^4 Pa), the temperature dependence of log G' versus log G'' plots begins to disappear. This is attributable to the fact that at high deformation rates, the application of oscillatory shear motion may disrupt and perhaps reform the network and the state of aggregation of polystyrene microdomains. The stable state at rest or at very low deformation rates will be a state where the molecualr network remains essentially intact. This now explains why in Figures 6 and 9 the temperature dependence of log G' versus log G'' plots diminishes as G'' is increased above a certain critical value. It is therefore important to remember that when comparing the T_r of a block copolymer determined from log G' versus log G'' plots with that determined from the SAXS technique, the dynamic viscoelastic data taken at low frequencies (i.e., $\omega \to 0$) is more appropriate than that taken at high frequencies for the discussion of the effect of temperature on the thermally induced order–disorder transition in block copolymers. Note that, as pointed out recently by Fredrickson and Larson,[38] terminal data also have critical anomaly. Under such circumstances, the values of T_r determined by log G' versus log G'' plots may not be very accurate.

Frequency–Temperature Superposition. In the past, a number of investigators[13-17] used frequency–temperature superposition to investigate the dynamic viscoelastic properties of SB, SIS, or SBS block copolymers in the temperature range over which the morphological change of block copolymers might have occurred (i.e., above the glass transition temperature of styrene domains). When the dependence of G' on temperature is different from that of G'', as is the case with Kraton 1102 and Kraton 1107 (see Figures 6 and 9), the use of frequency–temperature superposition is not justified. The fact that log G' versus log G'' plots vary with temperature clearly indicates that the block copolymer has different morphological states at different temperatures, and therefore the use of a shift factor for such materials is inappropriate. In other words, the use of frequency–temperature superposition is valid only for those situations where the morphological state of a polymer does not change with temperature. In this context, a serious question may be raised as to the validity of frequency–temperature superposition used by previous investigators.[13-16]

It is appropriate to mention, at this juncture, that Fesko and Tschoegl[52] have pointed out the deficiency of frequency–temperature superposition, by correlating the dynamic mechanical responses of SBS block copolymers measured at various temperatures ranging from −83 to 86 °C at frequencies between 0.1 and 1000 Hz, i.e., below the glass transition temperature (T_g) of polystyrene present in the SB block copolymers. In other words, the highest temperature investigated by them was too low to have had thermally induced order–disorder transition, discussed above, in SBS block copolymers. Fesko and Tschoegl ascribed their observation of the deficiency of frequency–temperature superposition to the thermorheologically complex nature of SBS block copolymers, by pointing out that the frequency-dependent shift factors $a_T(\omega)$ derived from different response functions can differ, i.e., log $a_T(\omega)$ for the storage compliance may be different from log $a_T(\omega)$ for the loss compliance.

The Sensitivity of log G' versus log G'' Plots of Block Copolymers to Their Morphological States. We have shown above that with increasing temperature, log G' versus log ω and log G'' versus log ω plots (see Figures 4 and 5 for Kraton 1102 and Figures 7 and 8 for Kraton 1107) show a continuously decreasing trend in G' and G'', whereas log G' versus log G'' plots (see Figure 6 for Kraton 1102 and Figure 9 for Kraton 1107) initially show a decreasing trend and then become *virtually* independent of

temperature at and above a certain critical value. We contend that the existence of such a critical temperature observed in log G' versus log G'' plots is a manifestation of the microdomain structure, which existed in the block copolymer at lower temperatures, disappearing completely at the critical temperature, giving rise to a homogeneous phase. This critical temperature is termed the order–disorder transition temperature T_r of a block copolymer.

The above observations lead us to conclude that the log G' versus log G'' plot is very sensitive to the morphological state of a block copolymer. A close examination of Figures 6 and 9 reveals some important differences between Kraton 1102 and Kraton 1107 in their morphological changes as the temperature is increased above the T_g of the polystyrene phase in the respective block copolymers. Specifically stated, we observe in Figure 9 that log G' versus log G'' plots for Kraton 1107 vary gradually with increasing temperature from 140 to 230 °C, whereas we observe in Figure 6 that log G' versus log G'' plots for Kraton 1102 seem to vary little with temperature until 200 °C, then suddenly changes as the temperature is increased from 200 to 220 °C, and finally become *virtually* independent of temperature at 220 °C and above. It should be remembered (see Figure 10) that Kraton 1102 has a cylindrical microdomain structure and Kraton 1107 has a spherical microdomain structure at room temperature. Therefore the differences observed between the two block copolymers in their rheological responses, in terms of log G' versus log G'' plots, may be attributable to the differences in their microdomain structures. It may be speculated that when heated, the cylindrical microdomain structure in Kraton 1102 may be sufficiently stable not to respond rheologically to a variation in temperature until the temperature reaches about 200 °C, whereas the spherical microdomain structure in Kraton 1107 may respond with great sensitivity to a variation in temperature.

Morphologically speaking, a variation in log G' versus log G'' plots with temperature can come from two sources, one from a variation of the amount of polystyrene microdomain structure present in the block copolymer and the other from a change in the morphological state of the microdomain structure (spheres, cylinders, or lamellae) as the temperature is increased or decreased. The first source is rather obvious because more polystyrene microdomains will be dissolved in the polydiene matrix with increasing temperature. But such an obvious expectation cannot explain why G' versus log G'' plots for Kraton 1102 (see Figure 6) do not vary with temperature until the temperature reaches about 200 °C. According to Leibler's theory,[4] the microdomain structure (lamellar, cylindrical, or spherical) of the ordered phase influences the T_r and a transition from the disordered phase to the lamellar structure passes through the spherical and then cylindrical structure when the temperature is decreased from a very high value (see Figure 3). Assuming that the microdomain morphology of Kraton 1102 changes from the cylindrical to spherical structure as the temperature is raised from room temperature, we have computed the T_r of Kraton 1102 for the spherical microdomain structure, using Leibler's theory, and found it to be 283 °C, which is about 8 °C higher than the T_r for the cylindrical structure (see Table II). However, we do not have experimental evidence to support whether or not indeed the microdomain structure changes from the cylindrical to spherical structure when the temperature is raised from room temperature to T_r, as predicted by Leibler.[4]

There is a different view that, the equilibrium morphology of a block copolymer is dependent solely upon its composition. For instance, very recently, Ohta and Kawasaki[53] have extended Leibler's theory and predicted the morphology of the ordered microstructure in block copolymers, by including the long-range interactions of the local monomer concentration fluctuations. Applying the narrow interphase approximation of Helfand and Wasserman,[29a] Ohta and Kawasaki[53] investigated the transition between different structures, namely, from lamellar to cylindrical microstructure and from cylindrical to spherical microstructure in the strong-segregation limit. They concluded that (1) a transition from lamellar to cylindrical structure occurs at $f_1 = 0.355$ and (2) a transition from cylindrical to spherical structure occurs at $f_1 = 0.215$, where f_1 is the volume fraction of polystyrene domains in a block copolymer. The microdomain structures of Kraton 1102 and Kraton 1107, displayed in Figure 10, are in agreement with this theoretical prediction. Note that f_1 is about 0.24 for Kraton 1102 and aboout 0.12 for Kraton 1107. It should be mentioned, however, that the microdomain structures reported experimentally in the literature and those in Figure 10 were determined at room temperature and therefore such experimental observations are not sufficient to dispel the possibility that the microdomain structure of a block copolymer can indeed vary with temperature, as predicted in Leibler's theory. This is an important area to be dealt with in future investigations.

Table IV
T_g, T_m, and the Heat of Fusion (ΔH_f) Determined from DSC Measurements for VAEOH Terpolymers

sample code	vinyl alcohol, mol %	T_g, °C	T_m, °C	ΔH_f, J/g
1	6	−6.0	*a*	*a*
2	14	−4.2	90.7	0.402
3	22	2.5	93.6	1.580
4	30	14.7	94.0	8.955

[a] Sample 1 is amorphous.

The Sensitivity of log G' versus log G'' Plots of Partially Crystalline Flexible Polymers to Temperature. In order to demonstrate how sensitive the log G' versus log G'' plot to the morphological state of partially crystalline flexible polymers is, let us consider the dynamic viscoelastic properties of partially hydrolyzed poly[(vinyl acetate)-*co*-ethylene] (VAE). Note that when the amount of vinyl acetate in the copolymer of vinyl acetate and ethylene is more than about 60 wt %, the copolymer is referred to as VAE, which is still amorphous. However, when hydroxyl groups are introduced into the backbond of the vinyl acetate in VAE, the resultant terpolymer, poly[(vinyl acetate)-*co*-ethylene-*co*-(vinyl alcohol)] (VAEOH), may become partially crystalline when the amount of the hydroxyl group exceeds a certain critical value. Very recently, Han et al.[22] have prepared VAEOH with varying amounts of hydroxyl group and Table IV gives a summary of the thermal properties of the four different grades of VAEOH prepared. In Table IV it can be seen that, among the four samples, sample 1 has the least amount of hydroxyl group and is amorphous, whereas the three other samples are partially crystalline with varying degrees of crystallinity.

Since the VAEOH terpolymers are flexible at room temperature, it is possible to measure their dynamic viscoelastic properties at room temperature. Figure 11 gives log G' versus log G'' plots for the four VAEOH samples listed in Table IV. It can be seen in Figure 11 that at a fixed value of G'', the value of G' increases with increasing degree of crystallinity. This is consistent with our expectation because the more crystalline a VAEOH, the greater its modulus will be. Note that at room temperature

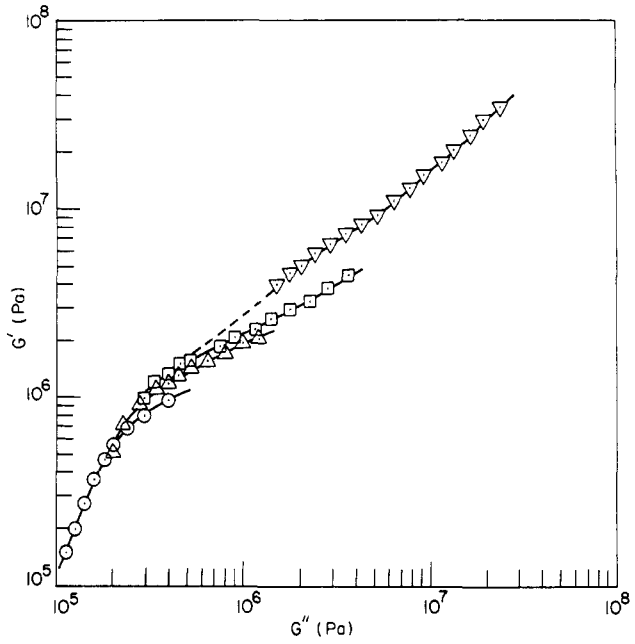

Figure 11. log G' versus log G'' plots at 25 °C for VAEOH terpolymer with different degrees of crystallinity:[22] (⊙) sample 1; (▲) sample 2; (⊡) sample 3; (▼) sample 4.

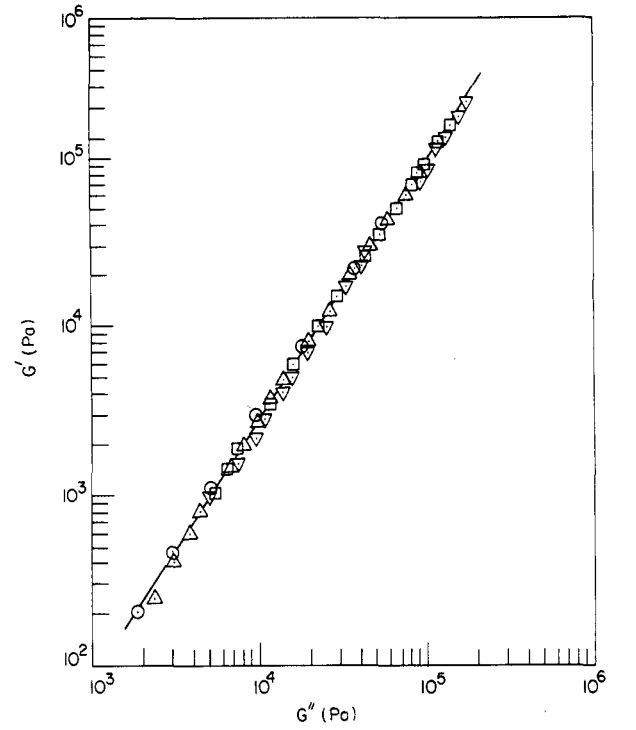

Figure 12. log G' versus log G'' plots at 100 °C for VAEOH terpolymers with different degrees of crystallinity.[22] Symbols are the same as in Figure 11.

samples 2, 3, and 4 have two phases, a crystalline phase being dispersed in an amorphous phase. We can, therefore, conclude that the log G' versus log G'' plots in Figure 11 show a sensitivity to the morphological state of the VAE-OH samples investigated.

However, when dynamic viscoelastic properties were measured at 100 °C, which is higher than the melting points of samples 2, 3, and 4 (see Table IV), log G' versus log G'' plots show *no* temperature dependence, as may be seen in Figure 12. Again, this is consistent with our expectation because all four samples have identical chemical structure and they form a homogeneous phase at temperatures above their melting points. The above results demonstrate once again that log G' versus log G'' plots are very sensitive to the morphological state of a flexible polymer, very similar to the situations observed above with the SBS and SIS block copolymers.

Conclusions

In the present investigation, we have utilized log G' versus log G'' plots in order to investigate the thermally induced order-disorder transition T_r of SBS and SIS block copolymers. We have defined T_r as the temperature at which log G' versus log G'' plots for a block copolymer cease to vary as the temperature is increased above the glass temperature of polystyrene. Using this rheological technique, we have determined the T_r of Kraton 1102 to be 220 °C and the T_r of Kraton 1107 to be 230 °C to within ±10 °C.

Having confirmed that Kraton 1102 has a cylindrical microdomain structure and Kraton 1107 has a spherical microdomain structure, we have computed values of T_r, using the currently held theories of Helfand–Wasserman[3,29,33] and Leibler.[4] In the computation, we have assumed that the microdomain structure, observed for Kraton 1102 and Kraton 1107 at room temperature, does not vary with temperature and we have used different forms of the interaction parameter suggested in the literature. We have learned that the use of the interaction energy density Λ, advocated by Roe and co-workers,[9-11,46] has advantages over the use of the Flory–Huggins interaction parameter χ, in that the necessity for determining the reference volume V_{ref} and the polymerization index N can be avoided.

We have learned that Helfand–Wasserman's theory predicts values of T_r very close to the measured values for both Kraton 1102 and Kraton 1107, whereas Leibler's theory predicts the value of T_r for Kraton 1107 reasonably close to the measured value, but it overpredicts that for Kraton 1102. This leads us to conclude tentatively that Leibler's theory predicts the T_r for spherical microdomain structures better than that for cylindrical microdomain structures, whereas Helfand–Wasserman's theory satisfactorily predicts T_r for both spherical and cylindrical microdomain structures. It is fair to say that Leibler's theory has no adjustable parameters, whereas Helfand–Wasserman's theory has many adjustable parameters (for example, see Table I). The present study indicates that an accurate determination of the interaction parameter and the temperature-dependent specific volumes is very important to successful predictions of the phase transition temperature of block copolymers, using the currently held theories.

It should be mentioned that the range of temperatures over which the thermally induced order–disorder transition takes place in an SB, SBS, or SIS block copolymer depends very much on its block lengths, styrene content, which in turn determines the morphological state of the block copolymers, and molecular weights. Therefore the range of transition temperatures obtained for the Kraton 1102 and Kraton 1107 in this study should not be construed to be applicable to other block copolymers having different block lengths, styrene content, or molecular weights. In future publications, we will discuss the effects of these variables on the order–disorder transition in SB, SBS, and SIS block copolymers.

Acknowledgment. We acknowledge that this study was made possible by a grant from the Exxon Education Foundation to the Polymer Science and Engineering Program at Polytechnic University and that Shell De-

velopment Co. supplied us with the block copolymers used in this investigation.

Registry No. (S)(I) (block copolymer), 105729-79-1.

References and Notes

(1) Meier, D. J. In *Block and Graft Copolymers*; Burke, J. J., Weiss, V., Eds.; Syracuse University: Syracuse, NY, 1973; p 105.
(2) Gallot, R. B. *Adv. Polym. Sci.* **1978**, *29*, 85.
(3) Helfand, E.; Wasserman, Z. R. *Macromolecules* **1978**, *11*, 960.
(4) Leibler, L. *Macromolecules* **1980**, *13*, 1602.
(5) Fredrickson, G. H.; Helfand, E. *J. Chem. Phys.* **1987**, *81*, 697.
(6) Hashimoto, T.; Tsukahara, Y.; Kawai, H. *J. Polym. Sci., Polym. Lett. Ed.* **1980**, *18*, 585.
(7) Hashimoto, T.; Shibayama, M.; Kawai, H.; Watanabe, H.; Kotaka, T. *Macromolecules* **1983**, *16*, 361.
(8) Hashimoto, T.; Kowsaka, K.; Shibayama, M.; Kawai, H. *Macromolecules* **1986**, *19*, 754.
(9) Roe, R. J.; Fishkis, M.; Chang, J. C. *Macromolecules* **1981**, *14*, 1091.
(10) Zin, W. C.; Roe, R. J. *Macromolecules* **1984**, *17*, 183.
(11) Nojima, S.; Roe, R. J. *Macromolecules* **1987**, *20*, 1866.
(12) Bates, F. S.; Hartney, M. A. *Macromolecules* **1985**, *18*, 2478.
(13) Chung, C. I.; Gale, J. C. *J. Polym. Sci., Polym. Phys. Ed.* **1976**, *14*, 1149; Chung, C. I.; Lin, M. I. *J. Polym. Sci., Polym. Phys. Ed.* **1978**, *16*, 545.
(14) Gouinlock, E. V.; Porter, R. S. *Polym. Eng. Sci.* **1977**, *17*, 534.
(15) Futamura, S.; Meinecke, E. *Polym. Eng. Sci.* **1977**, *17*, 563.
(16) Widmaier, J. M.; Meyer, G. C. *J. Polym. Sci., Polym. Phys. Ed.* **1980**, *18*, 2217.
(17) Bates, F. S. *Macromolecules* **1984**, *17*, 2607.
(18) Han, C. D.; Kim, J. *J. Polym. Sci., Part B: Polym. Phys.* **1987**, *22*, 1741.
(19) Han, C. D.; Lem, K. W. *Polym. Eng. Rev.* **1983**, *2*, 135.
(20) Chuang, H. K.; Han, C. D. *J. Appl. Polym. Sci.* **1984**, *29*, 2205.
(21) Han, C. D.; Chuang, H. K. *J. Appl. Polym. Sci.* **1985**, *30*, 2431.
(22) Han, C. D.; Ma, Y. J.; Chu, S. G. *J. Appl. Polym. Sci.* **1986**, *32*, 2478.
(23) Han, C. D.; Jhon, M. S. *J. Appl. Polym. Sci.* **1986**, *32*, 3809.
(24) Cole, K. S.; Cole, R. H. *J. Chem. Phys.* **1941**, *9*, 341.
(25) Doi, M.; Edwards, S. F. *J. Chem. Soc., Faraday Trans. 2* **1978**, *74*, 1802, 1818.
(26) Reference 23 considered only a special case for $p = 1$ in eq 1 and 2, but eq 4 is for all values of p.
(27) Helfand, E. *Macromolecules* **1975**, *8*, 552.
(28) Helfand, E. *Acc. Chem. Res.* **1975**, *8*, 295.
(29) (a) Helfand, E.; Wasserman, Z. R. *Macromolecules* **1976**, *9*, 879. (b) *Polym. Eng. Sci.* **1977**, *17*, 535. (c) *Macromolecules* **1980**, *13*, 994.
(30) Meier, D. J. In *Thermoplastic Elastomers*; Legge, N. R., Holden, G., Schroeder, H., Eds.; Hanser: New York, 1987; Chapter 11.
(31) Noolandi, J.; Hong, K. M. *Ferroelectrics* **1980**, *30*, 117. Hong, K. M.; Noolandi, J. *Macromolecules* **1981**, *14*, 727.
(32) de Gennes, P.-G. *J. Phys. (Les Ulis, Fr.)* **1970**, *31*, 235.
(33) Helfand, E.; Wasserman, Z. R. In *Development in Block Copolymers*; Goodman, I., Ed.; Applied Science: New York, 1982; Chapter 4.
(34) Helfand, E.; Sapse, A. M. *J. Chem. Phys.* **1975**, *62*, 1327.
(35) Mori, K.; Tanaka, H.; Hashimoto, T. *Macromolecules* **1987**, *20*, 381.
(36) Supplied by Shell Development Co.
(37) Ferry, J. D. *Viscoelastic Properties of Polymers*, 3rd ed.; Wiley: New York, 1980.
(38) Fredrickson, G. H.; Larson, R. G. *J. Chem. Phys.* **1987**, *86*, 1553.
(39) Hashimoto, T.; Shibayama, M.; Kawai, H. *Macromolecules* **1983**, *16*, 1093.
(40) Hashimoto, T.; Tsukahara, Y.; Kawai, H. *Polym. J.* **1983**, *15*, 699.
(41) Keller, A.; Pedemonte, E.; Willmouth, F. M. *Kolloid Z., Z. Polym.* **1970**, *238*, 385.
(42) Dlugosz, J.; Keller, A.; Pedemonte, E. *Kolloid Z., Z. Polym.* **1970**, *242*, 1125.
(43) Pedemonte, E.; Turturro, A.; Bianchi, U.; Devetta, P. *Polymer* **1973**, *14*, 146.
(44) Fetters, L. J.; Meyer, B. H.; McIntire, D. *J. Appl. Polym. Sci.* **1972**, *10*, 2079.
(45) Hashimoto, T.; Nakamura, N.; Shibayama, M.; Izumi, A.; Kawai, H. *J. Macromol. Sci., Phys.* **1980**, *B17*, 389.
(46) Lin, J. L.; Roe, R. J. *Macromolecules* **1987**, *20*, 2168.
(47) Rounds, N. A. "Thermodynamics and Phase Equilibria of Polystyrene-Polydiene Binary Mixtures". Doctoral Dissertation, University of Akron, Akron, OH, 1971.
(48) Richardson, M. J.; Savill, N. G. *Polymer* **1977**, *18*, 3.
(49) Rigby, D.; Roe, R. J. *Macromolecules* **1986**, *19*, 721.
(50) Mori, K.; Hasegawa, H.; Hashimoto, T. *Polym. J.* **1985**, *17*, 799.
(51) This correlation was computed by us, using information on the specific volume for polyisoprene, 1.0953 cm^3/g at 25 °C, as a reference state, and the volume expansion coefficient, $(1/v)(\partial v/\partial T) = 6.70 \times 10^{-4}$ (1/K), given in: *Polymer Handbook*, 2nd ed.; Brandrup, J., Immergut, E. H., Eds.; Wiley: New York, 1975; p V-7.
(52) Fesko, D. G.; Tschoegl, N. W. *J. Polym. Sci., Part C* **1971**, *No. 35*, 51.
(53) Ohta, T.; Kawasaki, K. *Macromolecules* **1986**, *19*, 2621.

Comparative Study on the Mean-Field and Scaling Theories of Temperature–Concentration Dependence of Slightly Cross-Linked Gel Systems

Miklós Zrinyi and Ferenc Horkay*

Department of Colloid Science, Loránd Eötvös University, H-1088 Budapest, Puskin u. 11-13, Hungary. *Received December 17, 1987; Revised Manuscript Received May 20, 1988*

ABSTRACT: The temperature dependence of the concentration of loosely cross-linked polymer networks swollen to equilibrium in poor solvent has been studied. An attempt is made to compare the prediction of different theories with experimental results. It is shown that the classical James–Guth network theory gives almost the same result as the modern thermal blob theory. Both theories predict universal dependence if scaled concentration and scaled temperature are used. This dependence excludes the possibility of first-order phase transition in gels below the Θ point. The Flory–Hermans–Wall–Kuhn theory predicts a collapse phenomenon, which has not been observed in our experiments. The results exhibited by poly(vinyl acetate) networks of different cross-linking densities swollen in isopropyl alcohol are diametrically opposed to those predicted on the basis of the Flory–Hermans–Wall–Kuhn theory, while the agreement with the James–Guth and thermal blob theories is quite satisfactory.

Introduction

Considerable attention has been paid recently to the theoretical and experimental investigation of the influence of solvent power on the network properties.[1-13] It is predicted that under certain conditions, the swollen polymer networks undergo a first-order, coil–globula like phase transition marked by a sharp collapse of the gel.[1-7]

Despite the theoretical works, the predicted sharp transition, called collapse, has not yet been observed experimentally, at least for neutral gels. Although poly-

0024-9297/89/2222-0394$01.50/0